

1.6 Fourier Transform Method

The Fourier transform (FT) method requires considerably more mathematical background than did our earlier description of filtered back projection. It will provide

- the most effective known numerical procedure for tomographic image reconstruction,
- theoretical support of the BP method, and
- means of deriving Radon's inversion formula - a numerically impractical, but mathematically very compact closed-form expression for the exact reconstruction.

1.6.1 Analytical description.

We assume that the density of the object is represented by a function $f(x_1, x_2)$, where x_1 and x_2 stand for the two spatial directions. The Fourier transform method is a technique to obtain the 2-D Fourier transform

$$\hat{f}(\omega_1, \omega_2) = \frac{1}{(2\pi)^2} \int_{-\infty}^{\infty} \int_{-\infty}^{\infty} f(x_1, x_2) e^{-i\omega_1 x_1} e^{-i\omega_2 x_2} dx_1 dx_2 \quad (1)$$

from the scan data. The density function $f(x_1, x_2)$ can then be recovered through

$$f(x_1, x_2) = \int_{-\infty}^{\infty} \int_{-\infty}^{\infty} \hat{f}(\omega_1, \omega_2) e^{i\omega_1 x_1} e^{i\omega_2 x_2} d\omega_1 d\omega_2 \quad . \quad (2)$$

We will give two descriptions of how one can arrive at the FT method. The most heuristic one follows below. A more concise (but probably less intuitive) version is given in subsection 1.7.3.

The key step of turning the scan data into $\hat{f}(\omega_1, \omega_2)$ rests on two observations:

- **Noting what happens' if we send in the X-rays in one particular direction, say parallel to the x_1 -axis:**

Figure 1a illustrates how we obtain the scan data $g(x_2) = \int_{-\infty}^{\infty} f(x_1, x_2) dx_1$. Its 1-D Fourier transform is

$$\begin{aligned} \hat{g}(\omega_2) &= \frac{1}{2\pi} \int_{-\infty}^{\infty} g(x_2) e^{-i\omega_2 x_2} dx_2 = \frac{1}{2\pi} \int_{-\infty}^{\infty} \left[\int_{-\infty}^{\infty} f(x_1, x_2) dx_1 \right] e^{-i\omega_2 x_2} dx_2 = \\ &= \frac{1}{2\pi} \int_{-\infty}^{\infty} \int_{-\infty}^{\infty} f(x_1, x_2) e^{-i0x_1 - i\omega_2 x_2} dx_1 dx_2 = 2\pi \hat{f}(0, \omega_2) \quad , \end{aligned}$$

i.e. we have obtained $\hat{f}(\omega_1, \omega_2)$ along a vertical line through origin in the (ω_1, ω_2) -plane (cf. Figure 1 b).

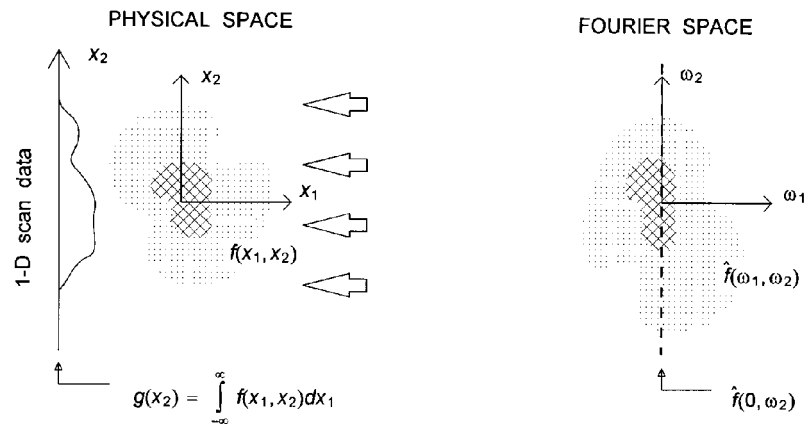


Figure 1 a,b. Recording with rays parallel to the x_1 - axis, and the corresponding data set in Fourier space.

- **Considering the difference, had the X-rays entered from a different direction:**

If the X-rays entered from an angle of θ (cf. Figure 1.3-2), the collected scan data will be exactly the same as if instead, the object had been turned an angle $-\theta$. As is shown in Section II.3.4 on Fourier transforms, turning an object turns its Fourier transform exactly the same angle. Therefore, we obtain in this case the values for $\hat{f}(\omega_1, \omega_2)$ along the line through the origin in the (ω_1, ω_2) - plane orthogonal to the X-ray direction in the physical plane. When we have taken X-ray images for $0 \leq \theta < \pi$, we have therefore obtained $\hat{f}(\omega_1, \omega_2)$ throughout the complete (ω_1, ω_2) -space. The density function $f(x_1, x_2)$ is then recovered by the 2-D Fourier transform (2).

Figure 2 sketches the steps required for collecting scan data and reconstructing the object using the FT method (also known as the projection slice theorem).

1.6.2 Numerical Description

Each of the 64 scan lines in Figure 1.3-1 contained 63 data points. We let these points correspond to x -values $[-\frac{N}{2} + 1, \dots, -1, 0, 1, \dots, \frac{N}{2} - 1]$ resp., and feed these to a complex FFT (which disregards the reflection frequency; cf. Section II.3.3) - without worrying anything about the implied periodicity of the data, relation between the continuous case and its discrete approximation etc. This produces 64 transformed scan lines, all complex, with real parts

symmetric and imaginary parts anti-symmetric, as seen in Figure 3 a,b. The next step is to lay out these lines with 1-D transform data radially in a 2-D (ω_1, ω_2) -plane. We then interpolate the numerical values to the Cartesian grid points, as indicated in Figure 4 (we need to determine the interpolation weights only in the highlighted octant - symmetries allow them to be re-used in the remaining seven octants). With second order (linear) interpolation, we get the (ω_1, ω_2) -plane data as seen in Figures 5 a,b. The 2-D (inverse) FFT produces the purely real reconstruction shown in Figure 6. This end result is purely real - down to the *rounding error* level of the computer (note that the *truncation error* level typically would be many orders of magnitude larger).

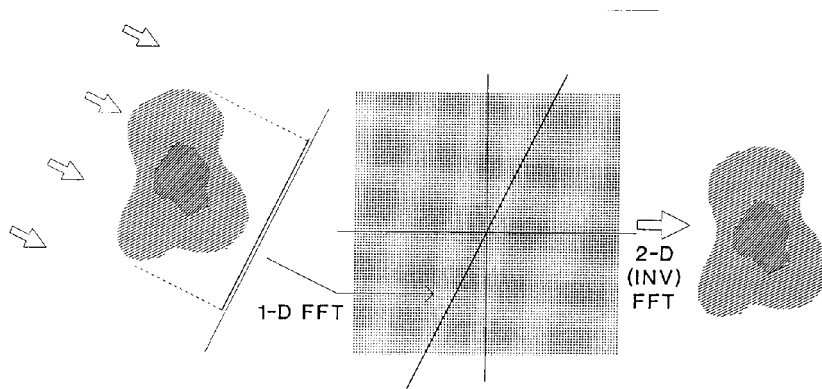


Figure 2. Schematic illustration of the four steps in the Fourier-based CT method:

- | | | |
|--------------------------|--|------------------------------------|
| 1. Measure attenuation | $p(x'_2)$ | } repeat for
different θ |
| 2. Calculate its 1-D FFT | $\hat{p}(\omega'_2)$ | |
| 3. Interpolate to get | $\hat{f}(\omega_1, \omega_2)$ | |
| 4. Invert by 2-D FFT | $f(x_1, x_2) = \text{reconstructed object.}$ | |

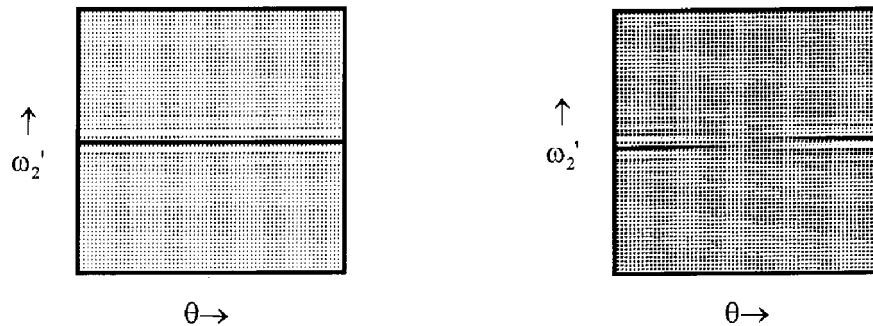


Figure 3. Real and imaginary parts that are obtained when 1-D FFTs have been applied to the scan lines.

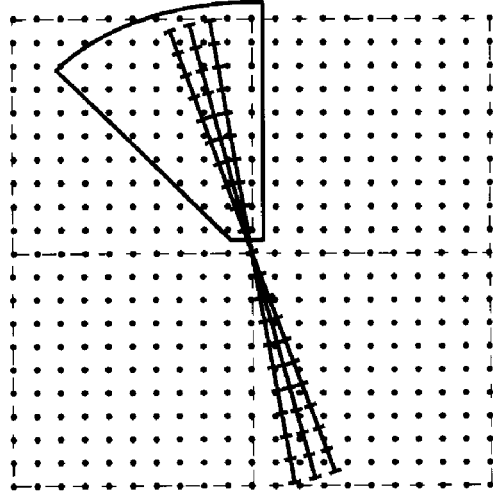
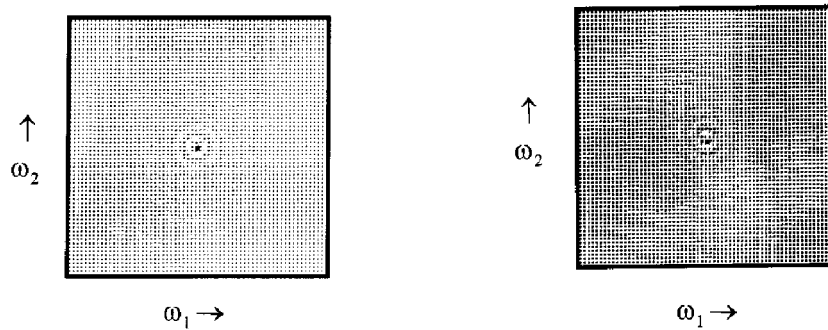
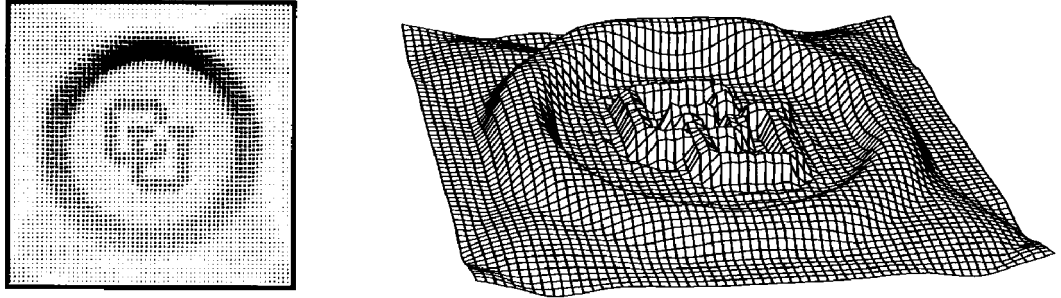


Figure 4. Interpolation from polar to Cartesian coordinates of the scan data in Fourier space. (Interpolation weights need only be calculated for octant 3 - symmetries allow them to be re-used in the remaining octants.)



Figures 5 a,b. Real and imaginary parts of the scan data when 1-D Fourier transformed, and interpolated to the (ω_1, ω_2) - plane.



Figures 6 a,b. Reconstructed image by the Fourier method.

We could similarly have started with a purely imaginary scan data set, and obtained a purely imaginary recovered image. With all steps being linear in the data values, two independent images can therefore be processed at one time using complex FFTs as described. This leads to comparable efficiency - but is far simpler algebraically - than using special codes for processing one image at a time.

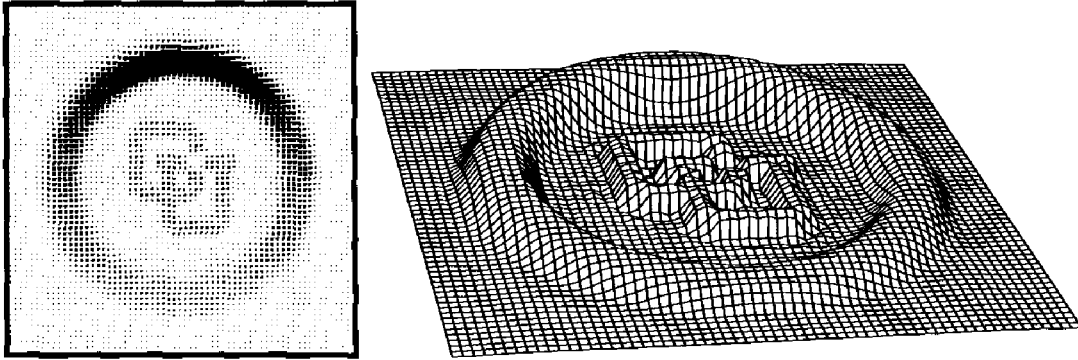
Back projection costs $O(n^3)$ operations per image (either when using a simple filter, as suggested in Section 1.5 or when the filter procedure for each line scan data is implemented via Fourier-based convolution as outlined in Section 1.7 - the dominant cost comes from the back-projection itself). For the FT method, the steps involving the 1-D FFTs, the interpolation, and the 2-D FFT cost $O(n^2 \log n)$, $O(n^2)$, and $O(n^2 \log n)$ operations respectively, for a much lower total of $O(n^2 \log n)$ operations.

1.6.3 Further Enhancements of Numerical FT Method

We can make several observations from Figures 3 and 5 that suggest how both computational efficiency and accuracy of reconstruction can be improved. From Figure 3, we can notice that the variation is far greater in the ω'_2 - than in the θ -direction. As a consequence, we can save a lot of work for little imaging loss by reducing the number of angular samples. Since the variation in the ω'_2 -direction is so great especially near the origin, second order interpolation is very inadequate. At least fourth order should be used.

In spite of the observations just made, the reconstruction in Figures 6 a,b shows a surprising clarity in detail. The most striking imaging error present is the low-mode undulations of

the background, most pronounced near the corners. Heuristically, this could be expected, since we are using periodic FFTs in place of infinite-domain transforms. Periodic images of the object are present near the boundaries of the shown domain. Discrepancies between the concept of periodicity in polar- and Cartesian coordinates account for a difficult-to-analyze error pattern. From this loose argument, one might expect that 'padding' (extension of the scan data by additional zeros on each side) would improve the image by increasing the distances to unphysical 'ghost'-images. For Figures 7 a,b, we have padded by a factor of two, i.e. doubled all array dimensions. The correction is seen to have been extremely effective - no visible error remains.



Figures 7 a,b. Same case as seen in Figures 6 a,b, but with the spatial domain 'padded' by a factor of two (i.e. doubled in size in each direction).

The significance of padding can be understood theoretically from a quite different approach than the one above (as noted by Gustafsson, 1996). Suppose we have a single Fourier mode $\sin nx$ and wish to interpolate it *in Fourier space* to a shifted grid in which the available modes are ... $\sin(-\frac{3x}{2})$, $\sin(-\frac{x}{2})$, $\sin \frac{x}{2}$, $\sin \frac{3x}{2}$, $\sin \frac{5x}{2}$, Second and fourth order interpolation suggests using

$$\begin{aligned} \frac{1}{2} \sin(n - \frac{1}{2})x + \frac{1}{2} \sin(n + \frac{1}{2})x &= (\sin nx) (\cos \frac{x}{2}) \\ -\frac{1}{16} \sin(n - \frac{3}{2})x + \frac{9}{16} \sin(n - \frac{1}{2})x + \frac{9}{16} \sin(n + \frac{1}{2})x - \frac{1}{16} \sin(n + \frac{3}{2})x &= (\sin nx) (\frac{9}{8} \cos \frac{x}{2} - \frac{1}{8} \cos \frac{3x}{2}) \end{aligned}$$

etc.

(cf. top two lines in Table III.2.-?).

We note:

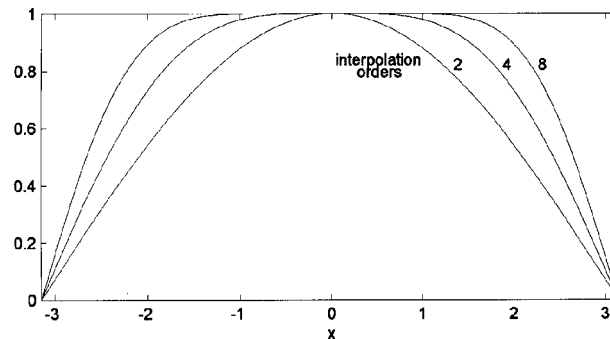
- i. Padding by a factor of two would in this case have entirely removed the interpolation errors (since no interpolation at all would then have been needed; additional frequencies, half-way between previously existing ones, would also have become available).

In general, the benefit of padding comes from the fact that it makes available more closely spaced frequencies. The interpolation takes place on a finer grid in frequency space, and is therefore more accurate. Still another way to justify padding is simply to note that a wider physical domain means that the actual image of interest becomes more central - a region in which errors are less, as we will see in a moment.

ii. It is very beneficial to increase the order of the interpolation.

For the frequency $\sin nx$ as input, we get in the test case back this initial frequency $\sin nx$, however damped with a factor that is 1 (i.e. no error) right at the domain center, but reduced to zero at its edge. Figure 8 shows how this damping factor approaches the ideal value 1 across an increasing interval as the interpolation order is increased.

Interpolation by order 4 and above achieves excellent result in the center of the domain; if used together with a factor 2 padding, we can expect near-perfect reconstruction (just as we saw in Figures 7 a,b).



Figures 8 a,b. The damping factor at different physical locations across the domain when an integer Fourier mode is interpolated in *Fourier space* to half-integer frequencies.

Both padding and increasing spatial numerical resolution lead to larger numerical grids. However, the operation count still remains $O(n^2 \log n)$ (and with a quite small proportionality constant). This is much superior to the $O(n^3)$ cost of filtered back projection. Techniques to further reduce costs within the FT method are at present an active field of research.